

THE USE OF X-RAY DIFFRACTION TO DETERMINE THE TRIAXIAL STRESS STATE IN CYLINDRICAL SPECIMENS

Paul S. Prevéy and Perry W. Mason
Lambda Research

ABSTRACT

A method of determining the axial, circumferential and radial residual stress distributions in cylindrical specimens is described. The axial and circumferential residual stresses are measured directly by x-ray diffraction at the free cylindrical surface exposed by machining and electropolishing. The radial stress component is then calculated from an integral of the circumferential stress at the free surface as a function of depth by the method of Moore and Evans.

The method is applicable only to cylindrical samples with rotationally symmetrical stress distributions from which complete cylindrical shells are removed for subsurface measurement. The method does not require prior knowledge of the stress-free lattice spacing, and thus provides a means of verifying neutron and x-ray diffraction methods of full tensor stress determination. The stress-free lattice constant, d_0 , is also calculated as a function of depth from the sum of the principal stresses.

Application of the method, to determine the triaxial residual stress distribution in an induction hardened 1045 steel multi-axial fatigue specimen, is described. The variation in the stress-free lattice spacing of the (211) planes with depth is estimated through the hardened case and into the core material.

INTRODUCTION

The classic $\sin^2\psi$ method of x-ray diffraction residual stress measurement (and the single-exposure and two-angle techniques derived from it) ⁽¹⁾ is based upon a model of plane stress at the free surface of the sample. No stress normal to the surface is assumed to exist in the thin layer (on the order of 10 μm) effectively penetrated by the x-ray beam. Subsurface

residual stress distributions are measured by removing layers of material in a manner which does not induce stresses. The stress distributions in directions lying in the plane tangent to the surface can be determined as a function of depth, provided stress relaxation caused by layer removal is trivial or can be calculated. Corrections for stress relaxation have been developed by Moore and Evans ⁽²⁾ for simple geometries and symmetrical stress fields.

The stress in the direction normal to the surface cannot generally be determined by x-ray diffraction using the plane stress model. Both x-ray and neutron diffraction techniques are available to determine the full stress tensor. However, the full stress tensor cannot be calculated without prior knowledge of the unstressed lattice spacing, d_0 . For many practical samples, the unstressed lattice spacing may be difficult to determine or composition-dependent, and vary with depth into the sample surface, as in carburized, nitrided or induction hardened steels.

In the singular case of cylindrical samples with rotationally symmetrical stresses, it is possible to determine the axial, circumferential and radial components of residual stress as functions of depth by applying the method of Moore and Evans, provided complete cylindrical shells are removed to expose each subsurface layer. The radial stress component is calculated as an integral of the circumferential stress measured on each exposed cylindrical surface as a function of depth.

As each cylindrical surface is exposed, the sum of the principal stresses can be determined and the value of the stress-free lattice spacing, d_0 , calculated (assuming plane stress at the exposed free surface) if the x-ray elastic constants are known. The variation in the stress-free lattice spacing with depth due to the carbon gradient and the percent martensite formed during heat treatment can then be determined.

Practical Applications of Residual Stress Technology, ed. C. Ruud, Materials Park, OH:
American Society for Metals, pp. 77-81

The method is of interest, not only for the determination of the three-dimensional stress distributions in cylindrical, rotationally symmetrical parts, but also as a means of independently determining the three dimensional stress state and the stress-free lattice spacing distribution for comparison to neutron and x-ray diffraction full-tensor stress measurement methods.

THEORY

Assuming a cylindrical sample (either a solid rod or a tube of inside radius R_1) with rotationally symmetrical stresses, Moore and Evans⁽²⁾ developed closed-form solutions for the true radial, axial and circumferential residual stress distributions at any radius r_1 calculated from only the circumferential and axial stress distributions measured as functions of depth by removing cylindrical shells:

$$\sigma_r(r_1) = - \left(1 - \frac{R_1^2}{r_1^2} \right) \int_{r_1}^R \left(\frac{r^2}{r^2 - R_1^2} \right) \frac{\sigma_{\theta_m}(r)}{r} dr \quad (1)$$

$$\sigma_z(r_1) = \sigma_{z_m}(r_1) - 2 \int_{r_1}^R \left(\frac{r^2}{r^2 - R_1^2} \right) \frac{\sigma_{2_m}(r)}{r} dr \quad (2)$$

$$\sigma_{\theta}(r_1) = \sigma_{\theta_m}(r_1) + \left(\frac{r_1^2 + R_1^2}{r_1^2 - R_1^2} \right) \sigma_r(r_1) \quad (3)$$

For the case of a solid bar, as in this application, R_1 equals zero. The radial stress component is calculated from the measured circumferential stress using Equation 1. The axial and circumferential stress distributions are corrected for stress relaxation caused by layer removal, using Equations 2 and 3.

Assuming that a condition of plane stress exists on the electropolished surface, free of any machining or grinding deformation, the lattice spacing will depend upon the stresses present in that surface as,

$$d(\psi) = \left(\frac{1+\nu}{E} \right) \sigma_{\phi} d_o \sin^2 \psi - \left(\frac{\nu}{E} \right) (\sigma_1 + \sigma_2) d_o + d_o \quad (4)$$

where ψ is the angle of tilt from the surface normal, σ_1 and σ_2 are the principal stresses, ν and E are Poisson's ratio and Young's Modulus, respectively, and d_o is the stress-free lattice spacing. Equation 4 is the basis for the $\sin^2 \psi$ method of residual stress determination by x-ray diffraction.

In the direction parallel to the surface normal, $\psi = 0$; therefore the observed lattice spacing depends only upon the sum of the principal stresses. Because the sum of the principal stresses equals the sum of any two perpendicular stresses, the sum of the circumferential and axial components may be substituted, and the unstressed lattice spacing is given by,

$$d_o = \frac{d(\psi=0)}{1 - \left(\frac{\nu}{E} \right) (\sigma_A + \sigma_c)} \quad (5)$$

where σ_A and σ_C are the axial and circumferential residual stresses measured on the free surface exposed by electropolishing. The x-ray elastic constants in the (hkl) direction of interest would generally be measured directly⁽³⁾. The value of d_o could be further corrected for systematic instrumental error, which was not undertaken in this investigation.

SAMPLE PREPARATION

The sample used in this study was prepared as part of the Society of Automotive Engineers Fatigue Design and Evaluation Committee's study of multi-axial fatigue life prediction. The sample was reportedly manufactured from induction hardened, hot rolled, 1045 steel, and was identified as sample 49X65601B. The sample had been fatigued to one-half of its anticipated cyclic life of 750,000 cycles in 5000 N·M multi-axial fatigue. The dimensions of the sample are shown in Figure 1.

The hardness distribution developed by induction hardening was measured on similar samples ⁽⁴⁾ and is depicted in Figure 2, indicating a hardened case depth on the order of nominally 4.5 mm.

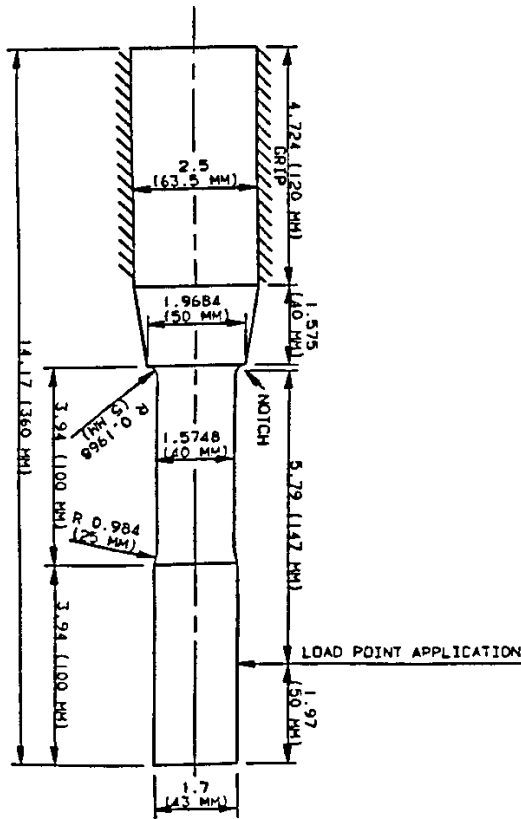


Fig. 1 - SAE 1045 steel induction hardened multi-axial fatigue sample

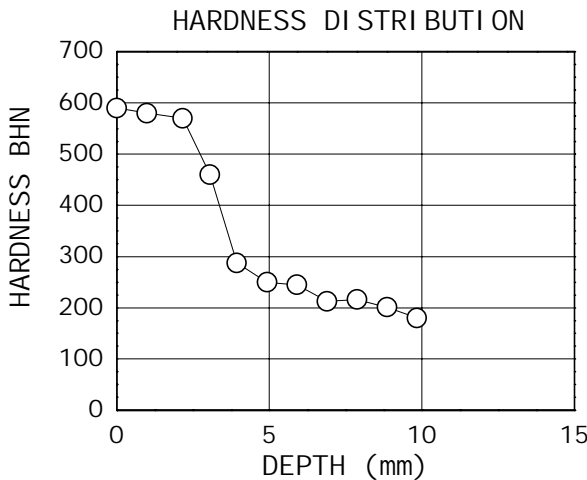


Fig. 2 - Brinnell hardness distribution through the induction hardened case

TECHNIQUE

Prior to x-ray diffraction measurement, the large grip end of the sample and the 100 mm extension were removed from either end of the cylindrical gage section to facilitate handling during machining and measurement. Stress relaxation, caused by sectioning to reduce the sample length, was assumed to be negligible.

X-ray diffraction residual stress measurements were made in the longitudinal and circumferential directions on the uniform cylindrical gage section at a location 10 mm from the point of tangency with the notch radius. Uniform cylindrical shells were removed from the gage section by first turning with a carbide tipped cutting tool, and then electropolishing to remove a minimum of 0.25 mm of material over a local area approximately 1.5 cm square to eliminate any residual stresses produced by turning.

X-ray diffraction residual stress measurements were performed using a two-angle technique employing the diffraction of chromium $K\alpha$ radiation from the (211) planes of the BCC structure of the 1045 steel. The diffraction peak angular positions at each of the ψ tilts employed for measurement were determined from the position of the $K\alpha_1$ diffraction peak separated from the superimposed $K\alpha$ doublet assuming a Pearson VII function diffraction peak profile in the high back-reflection region. ⁽⁵⁾ The diffracted intensity, peak breadth and position of the $K\alpha_1$ diffraction peak were determined by fitting the Pearson VII function peak profile by least squares regression after correction for the Lorentz polarization and absorption effects, and for a linearly sloping background intensity.

Measurements were performed on a computer-controlled Huber diffractometer, instrumented with a scintillation detector in a Bragg-Brentano geometry. The irradiated area was nominally 4 mm x 4 mm. The value of the x-ray elastic constant, $E/(1+\nu)$, required to calculate the macroscopic residual stress from the strain measured normal to the (211) planes of 1045 steel, was not determined during the course of this investigation. The data were reduced using constants previously determined for 1050 steel. ⁽³⁾

All data obtained as a function of depth were corrected for the effects of the penetration of the radiation employed for residual stress measurement into the

subsurface stress gradient.⁽⁶⁾ Systematic errors caused by instrument misalignment and sample displacement were monitored per ASTM E915, and found to be less than ± 14 MPa.

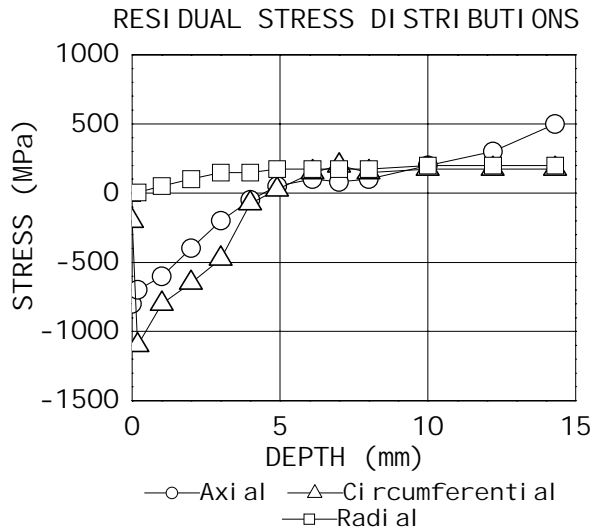


Fig. 3 - Triaxial stress distributions at a point 10 mm from the notch in the cylindrical gage section.

RESULTS AND DISCUSSION

The axial, circumferential and radial residual stress distributions are shown in Figure 3. The axial and circumferential results have been corrected using Equations 2 and 3, and the radial results are calculated from Equation 1.

The axial and circumferential stresses rise from maximum compression near the surface to cross into tension at a depth of nominally 4.5 mm. The axial stress reaches nominally 500 MPa at a depth of 14 mm.

The radial stress component is necessarily zero at the surface, and rises through the compressive case to reach a nearly constant value on the order of 180 MPa at a depth of approximately 5 mm.

The width of the (211) $K\alpha_1$ diffraction peak, separated from the $K\alpha$ doublet by Pearson VII peak profile fitting,⁽⁵⁾ is shown in Figure 4, without correction for instrumental broadening. The results show a sharp reduction in peak width at the surface, possibly the result of surface decarburization. In the hardened case,

the diffraction peak width is on the order of 5.8 deg. to a depth of nominally 2.5 mm. The peak width then diminishes rapidly through the remaining portion of the case to approach a uniform peak width of nominally 1.0 deg. in the soft core material. Comparison with the mechanically measured Brinnell hardness shown in Figure 2 indicates a similar trend. The sharp reduction in peak width at the surface is attributed to the shallow penetration of the x-ray beam, revealing a thin decarburized surface layer.

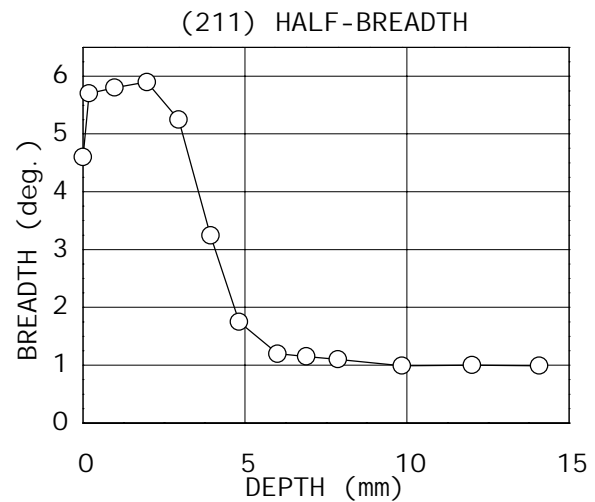


Fig. 4 - (211) diffraction peak width distribution

The subsurface distribution of the stress-free lattice spacing of the (211) planes, calculated from Equation 5, is shown in Figure 5. The results show a reduced lattice spacing near the surface, attributed to possible decarburization, followed by an increase in lattice spacing to nominally 1.1709 Å. The stress-free lattice spacing then diminishes with increasing depth through the case and reaches a value on the order of 1.1702 Å in the softer core material at a depth of nominally 5 mm. The variation in the lattice spacing within the core and the reduced lattice spacing immediately beneath the surface are not completely understood. The results presented are the average of three repeat measurements of the lattice spacing at $\psi = 0$, each with the sample repositioned. The experimental error estimated from the repeat measurement is $\pm 3 \times 10^{-5}$ Å. The variation observed in the core between depths of 5 mm and 14 mm appears to exceed the estimated experimental error.

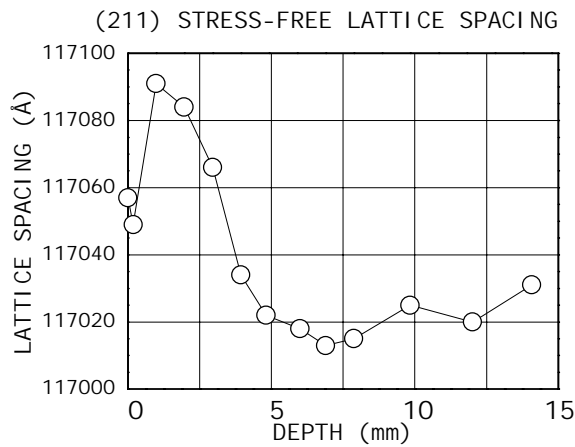


Fig. 5 - (211) stress-free lattice spacing distribution.

CONCLUSIONS

The method of correcting x-ray diffraction data for stress relaxation resulting from layer removal developed by Moore and Evans has been applied to determine the triaxial stress state throughout most of the volume of an induction hardened 1045 steel axle. The triaxial stress distributions obtained appear to correlate with the observed hardness variation, and provide for static equilibrium in the body.

A simple method of calculating the stress-free lattice spacing as a function of depth has been demonstrated. The results reveal a significant variation in the unstressed lattice spacing, d_0 , through the induction hardened case and into the core of the material.

The method described, generally applicable to any cylindrical specimen with rotationally symmetrical stresses, appears to provide a novel method of determining both triaxial stress and the stress-free lattice spacing distributions with depth for comparison to neutron and x-ray diffraction solutions of the full stress tensor.

ACKNOWLEDGEMENTS

The authors gratefully acknowledge the assistance of Mr. Thomas Cordes of the John Deere Corporation, and Dr. Peter Kurath of the University of Illinois, for providing the test sample, and Dr. Henry Prask of the NIST for discussion of the calculation of the stress-free lattice spacing.

REFERENCES

1. M. E. Hilley, ed., Residual Stress Measurement by X-ray Diffraction, SAE J784a, SAE, Warrendale, PA, 1971, p. 62.
2. M.G. Moore and W.P. Evans, Trans. SAE, Vol. 66, 1958, p. 340.
3. P. S. Prev y, *Adv. in X-ray Analysis*, Vol. 20, 1977, p. 345.
4. J.K. Oshsner, SAE Fatigue Design and Evaluation Committee Correspondence, June 1, 1988.
5. P.S. Prev y, *Adv. in X-ray Analysis*, Vol. 29, 1986, p. 103.
6. D.P. Koistinen and R.E. Marburger, Trans. ASM, Vol. 51, 1959, p. 537.